Light assisted solar fuel production by artificial CO_2 Reduction and water Oxidation

Deliverable D3.3

Optimized Fe_2TiO_5 photoanodes

Lead Beneficiary:	TUM
Work Package:	WP3
Delivery date:	31 August 2022
Type of deliverable:	Report
Dissemination level:	Public
Version:	v 1.0

This Project has received funding from the European Union's Horizon 2020 research and innovation programme under grant agreement No. 951843

Document Information

Grant Agreement Number	951843
Acronym	LICROX
Start date of the project (Duration)	01/09/2020 (36 months)
Document due date	31/08/2022
Submission date	31/08/2022
Authors	Ian Sharp
Deliverable number	D3.3
Deliverable name	Optimized Fe_2TiO_5 photoanodes
WP	WP3 – Semiconductors for the photo-anode and cathode

Version	Date	Author	Description
v.0	07/08/2022	Ian Sharp (TUM)	Creation of the first draft
v. 1.0	30/08/2022	Laura López (ICIQ)	Final document following final revision and approval by the Project Management Board

EXECUTIVE SUMMARY

This document is a public report that contains information about synthesis, characterization, and optimization of Fe_2TiO_5 photoanodes that are intended to serve as sustainable replacements for $BiVO_4$, offering all Earth-abundant elements, improved chemical stability, and reduced bandgap for use within the LICROX device. Given the confidential nature of the work, the specific synthesis conditions are discussed in general terms, more details are to be found in the confidential final review report. The basic structural and morphological properties of the electrodes and their representative performance characteristics are described. This report is a deliverable of the LICROX Project, which is funded by the European Union's H2020 Programme under Grant Agreement No. 951843. The Fe_2TiO_5 photoanodes are developed with the aim of later integration into the complete LICROX device and, together with the photocathode with coupled carbon dioxide reduction catalyst and organic photovoltaic solar cell component, will enable spontaneous overall CO_2 reduction to solar fuels.

Table of Contents

WP3: Semiconductors for the photo-anode and cathode 4
1. Purpose of the Optimized Fe_2TiO_5 Photoanodes (D3.3) 4
2. Synthesis and Characterization of Fe_2TiO_5 Photoanodes 4
3. Photoelectrochemical Characteristics of Fe_2TiO_5 Photoanodes 6
4. Conclusions and Future Prospects 7
5. References 7

WP3: Semiconductors for the photo-anode and cathode

By the implementation of WP3 we will target: i) The fabrication of highly efficient and stable $BiVO_4$ photoanodes as a model system that provides a basis for prototype development, ii) the development of high surface area WO_3 electron selective charge extraction layers fabricated from scalable NP dispersions; iii) the development of Fe_2TiO_5 photoanodes that overcome the fundamental limitations associate with $BiVO_4$; iv) the development of highly active and stable $CuFeO_2$ photoanodes; v) engineering photocathode structures and interfaces to enhance CO2R efficiency and C-C containing products selectivity; and vi) synthesis of semiconductor NPs for an up-scalable production of photo-anodes and cathodes.

1. Purpose of the Optimized Fe_2TiO_5 Photoanodes (D3.3)

The purpose of the optimized Fe_2TiO_5 photoanode is to absorb visible light as the wide bandgap top absorber of the LICROX device and to promote the charge transfer to water oxidation catalysts that will later be coupled to its surface. To accomplish these tasks with reasonable efficiency, high quality films must be produced that enable effective electron-hole charge separation, photocarrier transport, and interfacial hole injection. This is an emerging semiconductor material system and the development of a method for synthesizing high performance electrodes that are compatible with transparent conducting oxide back contacts is a major challenge. Although the LICROX device could alternatively operate using the previously developed $BiVO_4$ photoanode, Fe_2TiO_5 is developed, investigated, and assessed as a potential replacement because it comprises only Earth-abundant elements, has a narrower bandgap than $BiVO_4$ to enable enhanced absorption of sunlight, and is believed to offer superior photoelectrochemical stability.

2. Synthesis and Characterization of Fe_2TiO_5 Photoanodes

Two synthetic methods to produce Fe_2TiO_5 photoanodes have been pursued. In the first, films were prepared by spin-coating Fe_2TiO_5 nanoparticles from a suspension supplied by Avantama. Before deposition, some nanoparticle suspensions were subjected to a pre-annealing process to investigate the possibility of improved crystallinity in the resulting thin films. A spin speed of 1000 rpm was used, and a post-annealing process was used at elevated temperature. The development and synthesis of the suspensions are introduced in deliverable report D3.4. SEM images in Figure 1(a) and (b) show that, as desired, the nanoparticles agglomerate to form a continuous film after deposition and annealing. Additionally, the pre-annealed nanoparticles have a similar diameter (~21 nm) as non-pre-annealed particle films, but can easily aggregate and form larger gains. As displayed in Figure 1(c), clear X-ray diffraction peaks attributable to Fe_2TiO_5 only appear in the samples that are post-annealed at 800 °C, while lower annealing temperature that was tested (550 °C) did not cause Fe_2TiO_5 peaks to appear. Such lower temperatures are necessary for common transparent conductive oxides such as fluorine-doped tin oxide (FTO), which degrade at higher temperatures. The determined crystal phase of the Fe_2TiO_5 annealed at 800 °C is pseudobrookite, and the four highest diffraction peaks at 18.08, 25.53, 27.04 and 32.50° can be indexed to (200), (101), (111) and (230) planes according to literature[1].

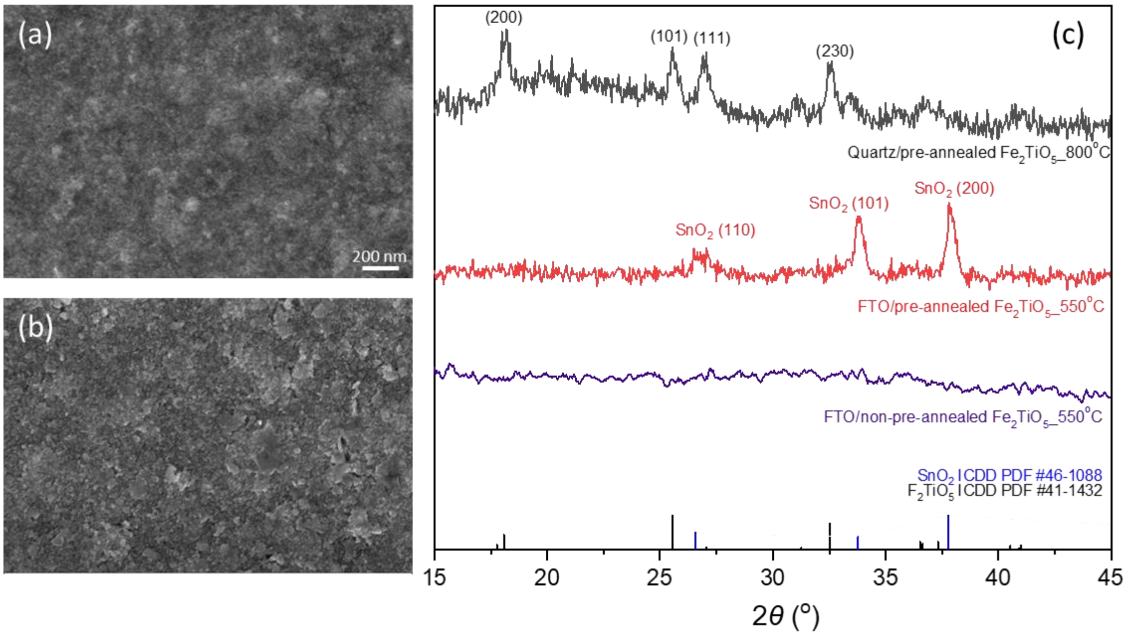

Figure 1. SEM images of (a) non-pre-annealed and (b) pre-annealed Fe_2TiO_5 nanoparticle films that were subsequently post-annealed at 550 °C. (c) XRD patterns of pre and non-pre-annealed Fe_2TiO_5 nanoparticle films that were post-annealed at 550 and 800 °C on FTO and fused silica substrates.

Sol-gel processing has also been used to produce Fe_2TiO_5 thin films, by spin coating a precursor solution. Various precursor concentrations of solution have been investigated along with different spin speeds to tune the thickness of the resulting film and attempt to control the crystalline orientation achieved during the post-deposition annealing process. SEM and AFM results show the topography of the sample (Figure 2a and 2b) and reveal the agglomeration of crystalline grains across the films; some defects can be noted. The effects of the post-annealing process on crystallinity were analyzed with XRD, the results are shown in Figure 2c. The Fe_2TiO_5 structure is confirmed after annealing, with peak intensity saturating after annealing at approximately 800 °C (samples fabricated with 850 °C annealing temperatures are shown in XRD plots). We observe that regardless of whether a slow 4 h temperature ramp in a muffle furnace or a rapid 10 s rapid thermal annealer (RTA) are used, a similar peak profile appears with noted Fe_2TiO_5 peaks as mentioned above. Annealing under vacuum conditions, however, produces Ti-doped hematite in agreement with other oxygen-derived Fe_2TiO_5 synthesis conditions noted in the literature[2]. Tauc analysis of UV-Vis absorption spectra (shown Figure 2d) shows a relatively linear increase in optical absorption across optical wavelengths, suggesting a high concentration of defects in the material. Fe-O and Ti-O transitions across the band gap can be noted, typical of Fe_2TiO_5 optical transitions noted in prior literature[3].

D3.3 Optimized Fe_2TiO_5 photoanodes

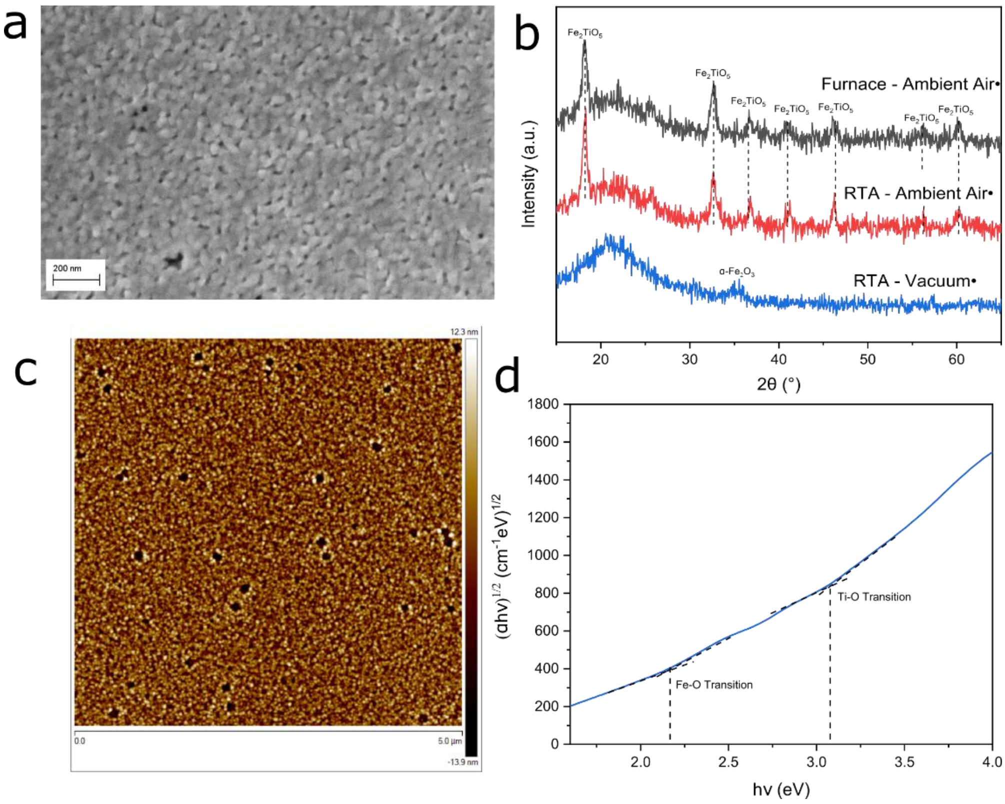

Figure 2. Characterization results of Fe_2TiO_5 thin films produced by sol-gel techniques, including (a) SEM images, (b) XRD plots showing the effects of different annealing conditions, (c) AFM topographic image, (d) Tauc analysis of UV-Vis absorption spectrum.

3. Photoelectrochemical Characteristics of Fe_2TiO_5 Photoanodes

Since FTO glass cannot withstand high-temperature (>600 °C) annealing, so far only the photoelectrochemical (PEC) performance of 550 °C post-annealed Fe_2TiO_5 nanoparticle photoanodes has been tested. Linear sweep voltammetry (LSV) was used for performance evaluation. Simulated sunlight was applied during a linear sweep of potential, and the induced current intensity shows the PEC activity. Prepared Fe_2TiO_5 films on FTO were measured in a three-electrode system, including a Fe_2TiO_5 photoanode, a Pt counter electrode, an Ag/AgCl reference electrode and a 0.1 M KOH electrolyte under simulated AM 1.5 irradiation. Further, in order to optimize the thickness of the films, a different number of spin-coating cycles was adopted. However, as shown in Figure 3, no photocurrent was detected for both samples with different thickness, which is believed to be a consequence of the poor crystallinity of the nanoparticles prepared at the lower post-annealing temperature. Therefore, it is crucial to find a type of transparent conductive substrate that is suitable for high temperature annealing for the future synthesis for both nanoparticle and sol-gel derived Fe_2TiO_5.

D3.3 Optimized Fe_2TiO_5 photoanodes

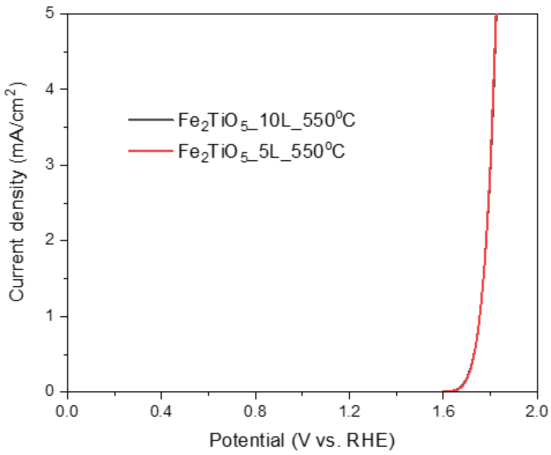

Figure 3. LSV curves of Fe_2TiO_5 photoanodes synthesized by five and ten-cycle-spin-coating cycles post-annealed at 550 °C measured in a three-electrode cell containing a photoanode, a Pt counter electrode and an Ag/AgCl reference electrode under one sun condition.

4. Conclusions and Future Prospects

Fe_2TiO_5 photoanodes based on thin films have been produced by nanoparticle and sol-gel methods, both with the use of spin coating. To date, structure optimization results in the formation of crystalline films of the targeted phase. One of the most crucial aspects for future work that has emerged is the need for synthesis techniques to adequately crystallize the Fe_2TiO_5 without severely affecting other materials in the device during elevated temperature annealing. We are currently investigating using rapid thermal annealing (RTA) to achieve this, which may avoid, for example, degrading the FTO layer during annealing.

5. References

1. L. Pauling, *Zeitschrift fuer Kristallographie* 73, (1930), 97-113
2. P.S Bassi, F. Xi, M. Kolbach, R. Gunder, I. Ahmet, R. van de Krol, S. Fiechter, *The Journal of Physical Chemistry C* 124, 67, (2020), 19911-19921
3. P.S. Bassi, S.Y. Chiam, J. Barber, L.H. Wong, *ACS Applied Materials & Interfaces* 6, 24, (2014), 22490-22495